IEEE Access
Multidisciplinary ⋮ Rapid Review ⋮ Open Access Journal

Received August 16, 2019, accepted September 11, 2019, date of publication September 18, 2019, date of current version October 1, 2019.

Digital Object Identifier 10.1109/ACCESS.2019.2941914

Dynamic Switch Control of Steering Modes for Four Wheel Independent Steering Rescue Vehicle

FEIXIANG XU, XINHUI LIU, WEI CHEN, AND CHEN ZHOU
School of Mechanical and Aerospace Engineering, Jilin University, Changchun 130022, China

Corresponding author: Wei Chen (chenwei_1979@126.com)

This work was supported by the National Key Research and Development Program of China under Grant 2016YFC0802904.

ABSTRACT For the sake of realizing dynamic switch among three steering modes for the four wheel independent steering (4WIS) rescue vehicle in the non-stop state, the switch control strategy and the optimized wheel switch trajectory are studied in this paper. Aiming at ensuring the constant turning radius of the 4WIS rescue vehicle in the switch process of steering modes, the steering angle relationships between the driving wheel and driven wheels are derived, and the desired driving wheel angle of the target steering mode is calculated. The B-spline curve is proposed to design the switch trajectory of the driving wheel. Two objectives including minimizing the sudden change of vehicle dynamic parameters and minimizing the energy consumption in the switch process are discussed. A multi-objective genetic algorithm (MOGA) based on non-dominated sorting genetic algorithm II (NSGA-II) is proposed to deal with the optimization problem of the wheel switch trajectory. The numerical simulations based on Matlab/Simulink indicate that the presented algorithm can generate the Pareto optimal solutions and is suitable for the optimization of the wheel switch trajectory. In addition, the proposed switch control strategy of steering modes for the 4WIS rescue vehicle in the non-stop state is validated to be reasonable and effective.

INDEX TERMS Four wheel independent steering (4WIS) rescue vehicle, dynamic switch of steering modes, constant turning radius, optimal switch trajectory, multi-objective genetic algorithm (MOGA).

I. INTRODUCTION

Rescue vehicles are playing a significant role in the disaster relief, patient assistance and the rescue materials transportation. A large number of governments around the world have strongly supported the development of rescue vehicles. Currently, rescue vehicles with the traditional front wheel steering (FWS) mode cannot successfully and quickly pass through narrow areas, such as urban villages, pedestrian streets and narrow lanes, leading to waste of rescue time seriously. In this context, a four wheel independent steering (4WIS) system of rescue vehicles is designed to achieve four steering modes, including FWS, rear wheel steering (RWS), four wheel steering (4WS) and in-situ steering. The passing and mobility of rescue vehicles in the narrow areas will be greatly improved through the switches among the four steering modes.

Lots of scholars have studied the control strategies and conducted experiments for the 4WIS vehicle [1]–[5]. Setiawan *et al.* [1]–[3] focused on the control strategies of path tracking and handing stability for the 4WIS vehicle, but they did not study the dynamic switch among multiple steering modes. Tu *et al.* [4] developed a 4WIS electric vehicle which steered by four steering modes including FWS, RWS, 4WS and in-situ steering, and they pointed out that the 4WIS electric vehicle has to be still completely when switching to other steering modes. Lam [5] designed a 4WIS agricultural mobile robot which can steer by way of FWS mode, RWS mode, 4WS mode and zero-radius steering mode, while the switch among steering modes requires the vehicle to be still. From most of the related researches currently, we can see that the 4WIS vehicle must be still when switching to other steering modes.

However, the switch among steering modes for the 4WIS rescue vehicle in the stationary state has some drawbacks as follows: (1) the stationary state restricts the driving mobility of the 4WIS rescue vehicle;(2) the stationary state hinders the development of intelligent vehicles, for example unmanned autonomous vehicles;(3) the stationary state is complicated and time consuming for drivers;(4) the steering torque for the stationary vehicle is significantly greater than the running vehicle, which indicates that steering modes switches for

The associate editor coordinating the review of this manuscript and approving it for publication was Xiaosong Hu.

the 4WIS rescue vehicle in the parking state consume larger energy. To this end, it is necessary to study the dynamic switch of steering modes for the 4WIS rescue vehicle in the non-stop state.

Since the in-situ steering mode has to be completed in the parking sate, this paper studies the dynamic switch among FWS mode, RWS mode and 4WS mode for the 4WIS rescue vehicle in the non-stop state. In order to minimize the changes of driver's driving feeling and the vehicle's driving states after switching to other steering modes, the constant turning radius of the vehicle is used as the control target of the dynamic switch of steering modes in the non-parking state. Based on the constant turning radius principle and Ackerman's theorem, the steering angle relationships between the driving wheel and other three driven wheels during the switch process are derived, and the desired angle of the driving wheel of the target steering mode is calculated. Another most important step for dynamic switch of steering modes is to design the switch trajectories of four wheels.

At present, the trajectory planning mainly adopts arc-line [6], Bezier curve [7], [8], polynomial curve [9] and B-spline curve [10], [11]. The arc-line based wheel trajectory planning method is easy to implement, but the curvature is discontinuous at the line and arc connection, causing the mutations of the vehicle dynamic parameters. The wheel trajectory based on the Bezier curve can solve the problem of arc-line discontinuity, but the calculation process is very cumbersome. The polynomial curve is not suitable for designing the wheel trajectory because of its lack of flexibility in curve variation. Based on the advantages of flexible curve change, easy implementation and continuous curvature [12], B-spline theory is used to construct the switch trajectories of wheels for the 4WIS rescue vehicle.

The switch trajectories of wheels determine the dynamic performance and energy consumption of the 4WIS rescue vehicle in the switch process. In order to obtain the optimal switch trajectory, the optimal goals are proposed in this paper. On the one hand, the change of the wheel angle with the steering mode switch causes the variation of kinetic parameters of the 4WIS rescue vehicle, which influences the dynamic performance of the 4WIS rescue vehicle. The lateral acceleration can reflect the roll stability of the vehicle, thus its' maximum change rate during the switch process is used as an optimization target to improve the wheel trajectory. On the other hand, the 4WIS rescue vehicle consumes energy during the steering mode switch process, so the tire dissipation energy is used as another objective.

The optimization of wheel trajectory in this paper belongs to the multi-objective optimization problem. Some scholars adopt the weighted objective function method to transform the multi-objective optimization problem into a single-objective optimization problem. However, the single-objective optimization algorithm based on the weighted objective function method has two shortcomings: (1) it cannot assign effective weights reasonably because of different dimensions of two objectives mentioned above; (2) it is sensitive to the shape of the Pareto front and cannot handle the non-convex Pareto front [13]. The multi-objective optimization algorithm does not have a single solution that can satisfy all the optimal targets at the same time [14], and it can obtain a set of Pareto optimal solutions. Users can choose one or a set of solutions as the final solution in the multi-objective optimization problem according to their preferences. Hence, a multi-objective genetic algorithm (MOGA) is put forward. Non-dominated soring genetic algorithm (NSGA-II) is widely used to solve the MOGA problem [15]–[19], and its computational complexity is acceptable. In NSGA-II, each generation of elites is retained to accelerate the performance of the MOGA [20]. Therefore, a MOGA based on NSGA-II is proposed in this paper to obtain the optimal wheel trajectory of steering mode switch.

The research in this paper has the following innovations and highlights.

(1) Aiming at dealing with the shortcomings of steering modes switch for the 4WIS rescue vehicle in the parking state, the dynamic switch control strategy in the non-stop state based on the constant turning radius principle is proposed.

(2) Based on the B-spline theory, the wheel switch trajectory of the 4WIS rescue vehicle is constructed.

(3) Two optimization objectives including the maximum change rate of the lateral acceleration and the tire dissipation energy are put forward, and a MOGA based on NSGA-II is proposed to obtain the optimal wheel switch trajectory.

The rest of this paper is organized as follows: Section 2 focuses on the dynamic switch control strategy of steering modes for the 4WIS rescue vehicle in the non-stop state. Section 3 designs a MOGA based on NSGA-II to obtain the optimal wheel switch trajectory; Section 4 describes the numerical simulations to validate the proposed switch method of steering modes; and the final section is the conclusions and the further work.

II. DYNAMIC SWITCH CONTROL STRATEGY OF STEERING MODES FOR THE 4WIS RESCUE VEHICLE

In order to reduce the changes of driver's driving sense and vehicle driving state before and after switching to other steering modes, keeping the turning radius of the vehicle unchanged is set as the control target in the steering mode switch period, and the switch control among FWS mode, RWS mode and 4WS mode for the 4WIS vehicle in the non-stop state is realized. The steering mode is switched by the driver pressing the button in the cab. The steering mode switch control flowchart for the 4WIS rescue vehicle is shown in Figure 1.

Firstly, the turning radius before the steering mode switch is calculated by collecting the angle sensor value of the front right wheel or the rear right wheel. Secondly, based on the constant steering radius principle, the relationships between the three driven wheels and the driving wheel during the switch process are calculated, at the same time, the target steering angle of the driving wheel is obtained according to the target steering mode which is acquired by switch

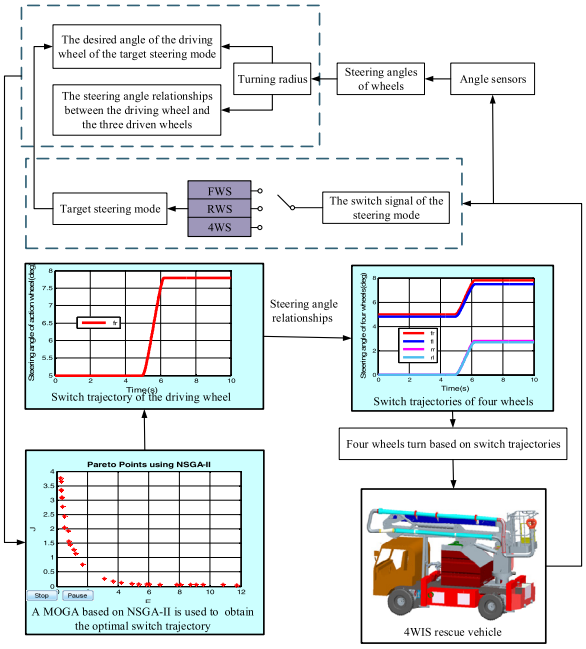

FIGURE 1. The steering mode switch control flowchart for the 4WIS rescue vehicle.

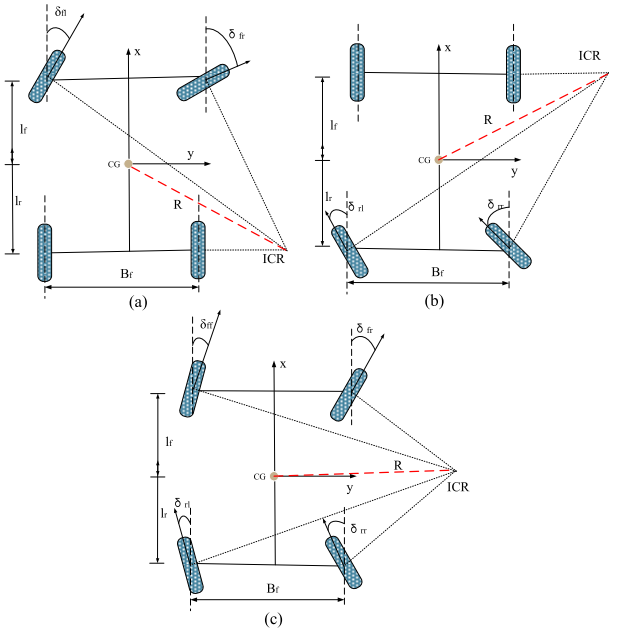

FIGURE 2. Three steering modes based on Ackerman's theorem: (a) FWS mode; (b) RWS mode; (3) 4WS mode.

signal of the steering mode. In this paper, the steering angle is defined as positive when the vehicle turns clockwise. When the vehicle turns clockwise, the front right wheel of the vehicle is set as the driving wheel; when the vehicle turns counterclockwise, the front left wheel of the vehicle is set as the driving wheel. After the driving wheel is determined, the remaining three wheels are defined as the driven wheels. Then, B-spline curve is used to construct the switch trajectory of the driving wheel, and it is optimized by a MOGA based on NGSA-II. Furthermore, according to the angle relationships between the three driven wheels and the driving wheel in the switch process, the switch trajectories of the three driven wheels are obtained. Finally, four wheels are controlled by four hydraulic cylinders independently to rotate at the same time based on the switch trajectories. Once the steering mode switch is finished, drivers can steer the vehicle in a new steering mode by manipulating the steering wheel.

A. TURNING RADIUS

When the vehicle is in the steering condition, all the wheels are required to be in the ideally pure rolling state. In other words, the steering angles of the wheels need to conform to the Ackerman theorem. Three steering modes based on Ackerman's theorem are shown in Figure 2. $\delta_{fl}, \delta_{fr}, \delta_{rl}, \delta_{rr}$ denote the steering angles of the front left wheel, the front right wheel, the rear left wheel and the rear right wheel, respectively. *ICR* is the instantaneous center of rotation. R is the turning radius. $l_f(l_r)$ represent the distance between the centroid and the front (rear) axle. B_f is the wheelbase.

As shown in Figure 2(a), when the vehicle steers by means of the FWS mode before switching to other steering modes, the turning radius is expressed as follows.

$$R = \sqrt{\left(\frac{l_f + l_r}{\tan\delta_{fr}} + \frac{B_f}{2}\right)^2 + l_r^2} \tag{1}$$

As shown in Figure 2(b), when the vehicle runs in the RWS mode before switching to other steering modes, the turning radius is shown as follows.

$$R = \sqrt{\left(\frac{l_f + l_r}{\tan(-\delta_{rr})} + \frac{B_f}{2}\right)^2 + l_f^2} \tag{2}$$

As shown in Figure 2(c), when the vehicle is in the 4WS mode before switching to other steering modes, the turning radius is displayed as follows.

$$R = \sqrt{\left(\frac{l_f + l_r}{(1-k)\delta_{fr}} + \frac{B_f}{2}\right)^2 + \left(\frac{l_r + kl_f}{1-k}\right)^2} \tag{3}$$

where k denotes the ratio of the rear wheel angle and the front wheel angle in the 4WS mode. In this paper, a simple control strategy for the 4WS mode of the vehicle is adopted to ensure that the yaw rate remains constant and the sideslip angle is zero, and k can be obtained as follows.

$$k = \frac{mV_x^2 l_f C_f + 2(l_f + l_r) l_r C_f C_r}{mV_x^2 l_r C_r + 2(l_f + l_r) l_f C_f C_r} \tag{4}$$

where m is the vehicle mass, V_x denotes the longitudinal speed of the vehicle, C_f, C_r represent the cornering stiffness of the front and rear tires, respectively.

B. RELATIONSHIP BETWEEN THE DRIVING WHEEL AND THE DRIVEN WHEELS DURING THE SWITCH PROCESS

As mentioned above, the front right wheel or front left wheel of the vehicle is set as the driving wheel, and the remaining three wheels are defined as the driven wheels.

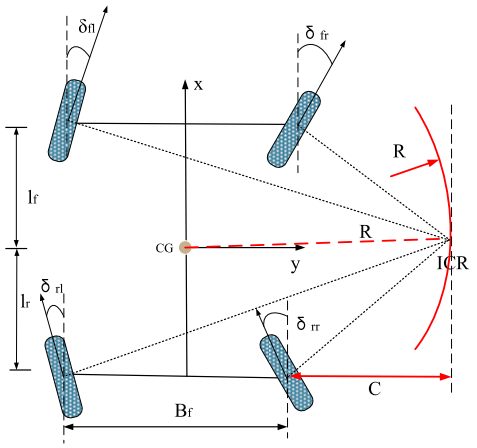

FIGURE 3. Movement of the instantaneous turning center during the switch process of the steering mode.

When the front right wheel is regarded as the driving wheel, based on the constant steering radius principle, the movement of the instantaneous turning center of the vehicle during the switch process is shown in Figure 3. The angle relationships between the three driven wheels and the driving wheel during the switch process of the steering mode are shown as follows.

$$\begin{aligned}\delta_{fl} &= \arctan\left(\frac{C\tan\delta_{fr}}{C+B_f}\right)\\ \delta_{rr} &= \arctan\left(\tan\delta_{fr}-\frac{l_f+l_r}{C}\right)\\ \delta_{rl} &= \arctan\left(\frac{C\tan\delta_{fr}}{C+B_f}-\frac{l_f+l_r}{C+B_f}\right)\end{aligned} \tag{5}$$

where C represents the vertical distance between the instantaneous turning center and the connection line between the front right wheel and the rear right wheel.

As shown in Figure 3, C can be calculated by the constant steering radius and the steering angle of the driving wheel, and the relationship among them is shown as follows.

$$C = \frac{\sqrt{R^2-(C+B_f/2)^2}}{\tan\delta_{fr}}+\frac{l_f}{\tan\delta_{fr}} \tag{6}$$

After reasoning, C can be calculated as follows in (7), as shown at the bottom of this page.

Similarly, when the front left wheel is set as the driving wheel, the angle relationships between the three driven wheels and the driving wheel during the switch process of the steering mode are shown as follows in (8), as shown at the bottom of this page

C. TARGET STEERING ANGLE OF THE DRIVING WHEEL

Based on the constant turning radius principle, the target steering angle of the driving wheel can be obtained.

As shown in Figure 2(a), when the target steering mode of the vehicle is FWS, the target steering angle *D_angle* of the driving wheel is expressed as follows.

$$D\_angle = \arctan\left(\frac{l_f+l_r}{\sqrt{R^2-l_r^2}-B_f/2}\right) \tag{9}$$

As shown in Figure 2(b), when the target steering mode is RWS, the target steering angle *D_angle* of the driving wheel is displayed as follows.

$$D\_angle = 0 \tag{10}$$

As shown in Figure 2(c), when the target steering mode is 4WS, the target steering angle *D_angle* of the driving wheel is shown as follows.

$$D\_angle = \frac{l_f+l_r}{1+k}\frac{1}{\sqrt{R^2-\left(\frac{l_r+kl_f}{1-k}\right)}-B_f/2} \tag{11}$$

$$C = \frac{-(B_f-2l_f\tan\delta_{fr})+\sqrt{(B-2l_f\tan\delta_{fr})^2-4(1+\tan^2\delta_{fr})(l_f^2+B_f^2/4-R^2)}}{2\left(1+\tan^2\delta_{fr}\right)} \tag{7}$$

$$\begin{aligned}\delta_{fl} &= \arctan\left(\frac{(C+B_f)\tan\delta_{fl}}{C}\right)\\ \delta_{rr} &= \arctan\left(\frac{C+B_f}{C}\tan\delta_{fl}-\frac{l_f+l_r}{C}\right)\\ \delta_{rl} &= \arctan\left(\tan\delta_{fl}-\frac{l_f+l_r}{C+B_f}\right)\\ C &= \frac{-(2B_f(\tan^2\delta_{fl}+1/2)-l_f\tan\delta_{fl})}{(1+\tan^2\delta_{fl})}\\ &\quad+\frac{\sqrt{(B_f(\tan^2\delta_{fl}+1/2)-l_f\tan\delta_{fl})^2-(1+\tan^2\delta_{fl})(l_f^2+B_f(\tan^2\delta_{fl}+1/4)-2B_fl_f\tan\delta_{fl}-R^2)}}{(1+\tan^2\delta_{fl})}\end{aligned} \tag{8}$$

III. OPTIMAL WHEEL SWITCH TRAJECTORY BASED ON MOGA

Based on the constant steering radius schema, the 4WIS rescue vehicle can realize the dynamic switch of steering modes without stopping. However, the switches among different steering modes can produce a sudden change of vehicle dynamics parameters, harming the safety of the 4WIS rescue vehicle. Therefore, it is essential to plan a smooth wheel trajectory during the steering mode switch process. The B-spline theory is applied to plan the driving wheel switch trajectory of the 4WIS rescue vehicle, and then the switch trajectories of the three driven wheels are obtained according to the angle relationships between the driven wheels and the driving wheel during the steering mode switch. In order to optimize the wheel switch trajectory based on B-spline curve, this paper adopts a MOGA to obtain a set of Pareto optimal solutions.

A. B-SPLINE CURVE

The B-spline curve is defined as follows [12].

$$Q(u) = \sum_{i=0}^{n} P_i N_{i,j}(u) \tag{12}$$

where j is the spline order, $P_i(i = 0, 1 \cdots n)$ is the $i-th$ control point of the B-spline curve, u denotes the node vector, $u_0 \le u_1 \le \cdots \le u_{n+j+1}$, $N_{i,j}(u)$ is $j-th$ basis function of the B-spline curve.

$N_{i,j}(u)$ is usually obtained using the Cox-de Boor recursive algorithm [22], and it is expressed as follows.

$$N_{i,0}(u) = \begin{cases} 1, & u_i \le u \le u_{i+1} \\ 0, & otherwise \end{cases} \tag{13}$$

$$N_{i,j}(u) = \frac{u - u_i}{u_{i+j} - u_i} N_{i,j-1}(u) + \frac{u_{i+j+1} - u}{u_{i+j+1} - u_{i+1}} N_{i+1,j-1}(u) \tag{14}$$

According to the node vectors u_i, u_{i+1}, first order basis functions of the B-spline curve are acquired using Equation (13).The basis functions of the higher orders from 2 to j are obtained through the recursive method shown in Equation (14). The basis functions of B-spline curve can control curve locally, allowing any trajectory segment to be modified without influencing the adjoining segments of the curve.

The continuity of the switch trajectory requires the B-spline curve to be differentiable at least twice, as a result, this paper designs the B-spline curve which satisfies $n = 3, j = 3$.

B. OPTIMAL B-SPLINE CURVE BASED ON MOGA

In this paper, the maximum change rate of the lateral acceleration and the tire dissipation energy are taken as two optimization goals for the switch trajectory. A MOGA based on NSGA-II is designed to solve Pareto optimal solutions. Users can select optimal switch trajectory from Pareto front according to their preferences.

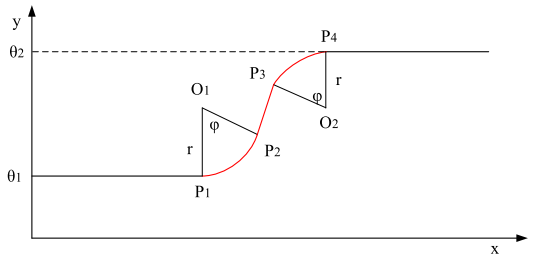

FIGURE 4. The design of control points based on the double circle tangent method.

1) MATHEMATICAL MODEL OF MOGA

In this section, the mathematical model of MOGA is presented.

a: OPTIMIZATION VARIABLE

Based on the analysis of equations (12)-(14), it is necessary to determine four control points to obtain a B-spline curve. This paper applies the double circle tangent method to obtain the control points of B-spline curve.

As shown in Figure 4, $P_1(t_1, \theta_1), P_2(x_2, y_2), P_3(x_3, y_3), P_4(t_2, \theta_2)$ are four control points of the B-spline curve, respectively. The x-axis represents the steering time, and the y-axis denotes the steering angle of the driving wheel. φ, r are the central angle and radius of the circle, respectively.

t_1, θ_1 are the steering time and steering angle before switching to other steering modes, respectively, which are known. θ_2 is the target steering angle of the target steering mode, and it can be calculated based on Equation 9-11. t_2 is the initial time after switching to the new steering mode. $P_2(x_2, y_2), P_3(x_3, y_3)$ and t_2 can be expressed as follows.

$$\begin{cases} x_2 = t_1 + r \sin\varphi \\ y_2 = \theta_1 + r - r\cos\varphi \\ x_3 = t_2 - r \sin\varphi \\ y_3 = \theta_2 - r + r\cos\varphi \\ t_2 = t_1 + \Delta t \end{cases} \tag{15}$$

It can be seen that control points of B-spline curve can be constructed with three variables $\varphi, r, \Delta t$. When the control points are described, the B-spline curve can be obtained based on equations (12)-(14). Hence, the design variables X of the B-spline curve optimization model is shown as follows.

$$X = (\varphi, r, \Delta t) \tag{16}$$

The ranges of the design variables are defined as follows.

$$0 \le \varphi \le \frac{\pi}{2}, 0 \le r \le \theta_2 - \theta_1, 0.1 \le \Delta t \le 2 \tag{17}$$

b: OBJECTIVE FUNCTIONS

Two optimization objectives including the maximum change rate of the lateral acceleration and the tire dissipation energy are built. The maximum change rate of the lateral acceleration is used to maintain the roll stability of the vehicle in the steering modes switch process, and the tire dissipation energy

is proposed to reduce the energy consumption caused by the switch of the steering modes.

The maximum change rate of the lateral acceleration is defined as follows.

$$f_1(X) = \max\left(\frac{da_y}{dt}\right) \tag{18}$$

where $a_y = (\dot{\beta} + r_0)V_x$, a_y is the lateral acceleration of the 4WIS rescue vehicle, β denotes the sideslip angle of the 4WIS rescue vehicle, and r_0 represents the yaw rate of the 4WIS rescue vehicle.

The sum of each tire dissipation energy is shown as follows.

$$f_2(X) = \int_0^{\Delta t} P dt \tag{19}$$

where P denotes the sum of four tires dissipation power, and it can be expressed as follows [23].

$$P = F_y V_y + M_z r_0 \tag{20}$$

where F_y is the sum of the lateral force of four tires, V_y is the lateral speed, and M_z denotes the sum of the yaw moments.

F_y and M_z are obtained as follows.

$$\begin{aligned} F_y &= m(\dot{V}_y + V_x r_0) + m_s h\ddot{\phi} \\ M_z &= I_z\dot{r} - I_{xz}\ddot{\phi} \end{aligned} \tag{21}$$

where m_s is the sprung mass of the 4WIS rescue vehicle, h is the height of the 4WIS rescue vehicle centroid, ϕ denotes the roll angle of the 4WIS rescue vehicle, I_z represents the momentum of inertia of the 4WIS rescue vehicle around vertical direction, and I_{xz} represents the momentum of inertia of the 4WIS rescue vehicle around longitudinal and vertical directions.

The objective function of the mathematical model of MOGA is given as follows.

$$\min(f_1(X), f_2(X)) \tag{22}$$

The variables mentioned above for solving two functions $f_1(X)$ and $f_2(X)$ can be obtained through constructing the nonlinear 8DOF vehicle model whose detailed modelling steps and some specification parameters can be seen in Ref [24].

c: PARETO OPTIMALITY

The mathematical model proposed in this paper belongs to the multi-objective optimization problem, in which there is no single result can optimize multiple targets at the same time. The major reason is that multiple goals conflict with each other, in other words, one goal becomes worse with the optimization of the other goals. Therefore, the Pareto optimality concept is important in solving the multi-objective optimization problem.

For multi-objective optimization problems $f = \{f_1, f_2, \ldots f_q\}$, given a set of feasible solutions $X = [x_1, x_2 \ldots x_n]$, find a vector X^* that minimizes the given problem.

$$\min f(X) = \{f_1(X), f_2(X), \ldots f_q(X)\}, \quad X \in \Omega \tag{23}$$

where Ω is the solution space.

Given two feasible solutions $X_a \in \Omega, X_b \in \Omega$, if and only if

$$\forall i, \quad f_i(X_a) \leq f_i(X_b), \ i \in (1, 2, \ldots q) \tag{24}$$

and

$$\exists i, \quad f_i(X_a) < f_i(X_b) \tag{25}$$

X_a is said to dominate another feasible solution X_b, which is represented by $X_a < X_b$.

If a feasible solution is not dominated by any other solution in the solution space, then this solution is called the Pareto optimal solution. It can be seen from equations (24) and (25) that the Pareto optimal solution cannot optimize one of the targets and cause other targets to deteriorate. The set of all feasible non-dominant solutions in the solution space is called the Pareto optimal set or Pareto front.

2) DESIGN OF MOGA BASED ON NSGA-II

Genetic algorithms solve the global optimization problems by means of natural evolutionary criteria and are widely used in the optimization field [25]–[27]. However, genetic algorithms can only solve the single-objective optimization problem, and cannot directly obtain the Pareto optimal solutions [28]. The MOGA based on NGSA-II can deal with the true Pareto front [13] to get the optimal B-spline curve.

NGSA-II adopts the fast non-dominated sorting mechanism to make the optimization results converge the Pareto front. By defining the congestion degree and congestion comparison operators, the diversity of Pareto optimal solutions is guaranteed, and the elite strategy is introduced to expand the sampling space. The congestion distance refers to the intensity of individuals in the Pareto optimal solutions. The larger the congestion distance, the more uniform the individual distribution. The complexity of the NGSA-II algorithm is $O(qP_s^2)$ (q is the numbers of optimization targets and P_s is the population size).

The flowchart of the proposed MOGA based on NSGA-II is shown in Figure 5.

Step 1. The initial population is randomly generated.

Step 2. The new offspring population is generated based on the genetic algorithms' basic operations including selection, crossover and mutation.

Step 3. After merging the parent population with the offspring population, two objectives values including the lateral acceleration's maximum change rate and the tire dissipation energy are calculated.

Step 4. The fast non-dominated sorting and the degree calculation for each individual in the non-dominated layer are performed, and then the suitable individuals to form a new parent population is selected.

Step 5. Determining if the maximum genetic generation is reached, if not, return to step 2; otherwise the Pareto optimal solutions are achieved.

The parameters of the MOGA based on NGSA-II are set in Table 1.

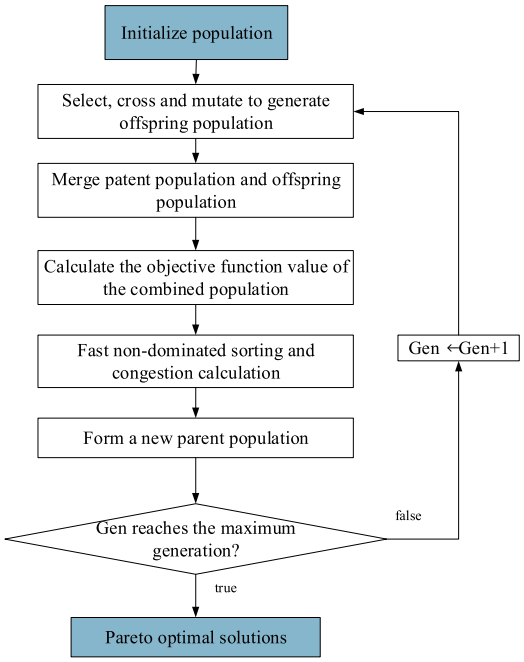

FIGURE 5. The flowchart of the proposed MOGA based on NSGA-II.

TABLE 1. Parameters for the MOGA based on NGSA-II.

Symbol	Parameter name	Value
P_s	Population size	100
N_g	Number of generations	30
P_c	Crossover probability	0.5
P_m	Mutation probability	0.2

IV. SIMULATIONS

Taking a 4WIS fire rescue prototype vehicle as an example, the numerical simulations based on Matlab/Simulink software are carried out to verify the effectiveness of the proposed dynamic switch of steering modes. There are six switches among FWS, RWS and 4WS. In this section, two typical switches from FWS to 4WS or to RWS are studied.

A. SWITCH FROM FWS TO 4WS

The longitudinal speed of the vehicle is set as 10 m/s and the road friction coefficient is set as 0.85 when the steering mode is switched from FWS to 4WS in this paper. The optimal switch trajectory of the driving wheel is obtained through the Pareto optimal solutions according to the MOGA based on NGSA-II, as shown in Figure 6. The users can select the corresponding optimization result according to their own experience or requirement.

The smaller $f_1(X)$, the smaller the sudden change of the lateral acceleration; and the smaller $f_2(X)$, the smaller the tire dissipation energy. Based on the actual requirements of the 4WIS fire rescue prototype vehicle, some optimization results from the Pareto optimal solutions are selected, which are listed in table 2.

Putting $X = (1.53, 0.50, 1.33)$ result into constructing the control points of the B-spline curve, and then an optimal

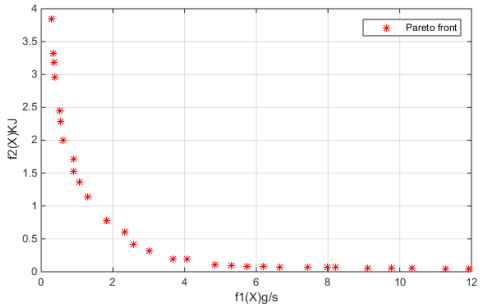

FIGURE 6. The Pareto optimal solutions during the switch process from FWS to 4WS.

TABLE 2. The selected optimization results from the Pareto optimal solutions.

Optimization variable X			$f_1(X)(m/s^3)$	$f_2(X)(KJ)$
$\varphi(rad)$	$r(\deg)$	$\Delta t(s)$		
1.44	0.70	1.40	0.51	2.45
1.56	0.55	1.21	0.62	1.99
1.44	0.43	1.01	0.91	1.53
0.48	0.45	0.60	2.32	0.60
1.53	0.50	1.33	0.54	2.29
0.66	0.34	0.68	1.82	0.78
0.37	0.15	0.50	2.57	0.42

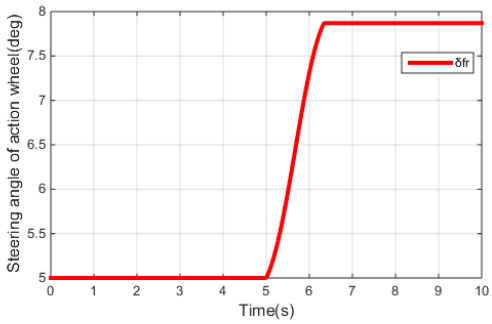

FIGURE 7. The steering angle of the driving wheel under the switch from FWS to 4WS.

switch trajectory of the driving wheel based on the B-spline curve is generated, as shown in Figure 7. The switch process can be seen in 5-6.33s period.

Further, based on the angle relationships between the driving wheel and the driven wheels during the switch process, the switch trajectories of four wheels are constructed, as shown in Figure 8. It shows that the vehicle runs in FWS mode in 0-5s period, and the vehicle is in the steering mode switch process in 5-6.33s period, and the vehicle is in 4WS mode in 6.33-10s period. During the switch process of steering mode, the calculated turning radius of the 4WIS fire rescue prototype vehicle remains constant at 35.1m, which

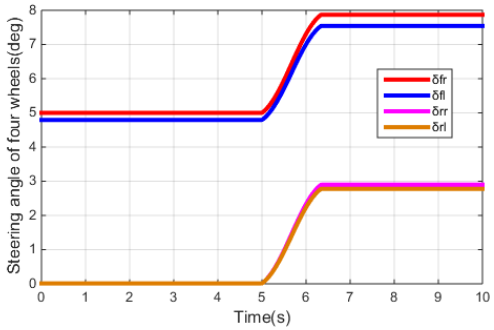

FIGURE 8. The steering angles of the four wheels under the switch from FWS to 4WS.

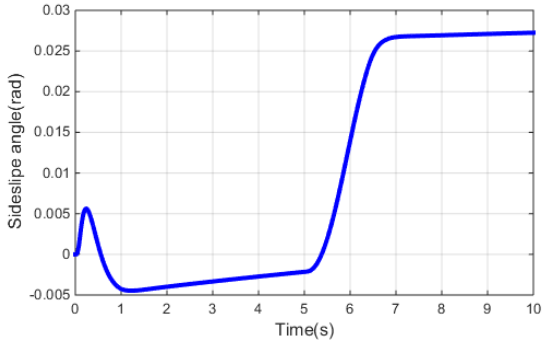

FIGURE 9. The sideslip angle response of the vehicle under the switch from FWS to 4WS.

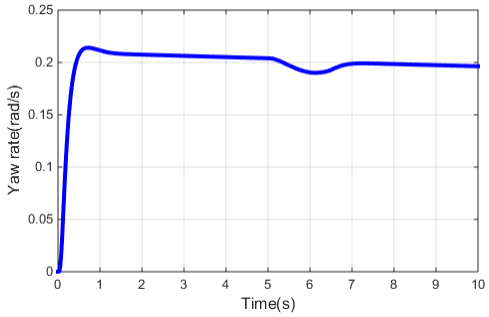

FIGURE 10. The yaw rate response of the vehicle under the switch from FWS to 4WS.

realizes the switch control target keeping the turning radius of the vehicle unchanged.

Taking the steering angles of four wheels as the input of the steering system, the simulation based on the 8DOF vehicle model is performed. The dynamic parameters of the 4WIS fire rescue prototype vehicle are shown in Figure 9-11.

As can be seen from Figure 9-10, during the 5-6.33s switch process from FWS to 4WS, the sideslip angle and the yaw rate of the 4WIS fire rescue vehicle change slowly, avoiding the parameters mutation caused by the switch of steering mode. In addition, Figure 11 shows that the smooth lateral acceleration guarantees the roll stability of the 4WIS fire rescue vehicle in the switch process. Therefore, the simulation results demonstrate that the proposed dynamic switch from FWS to 4WS is reasonable and effective.

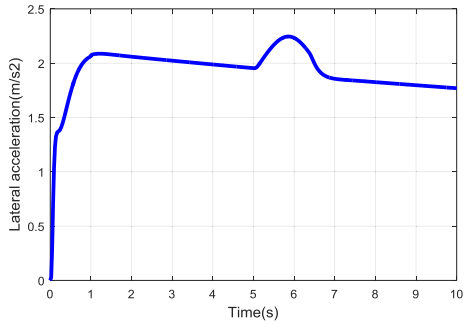

FIGURE 11. The lateral acceleration response of the vehicle under the switch from FWS to 4WS.

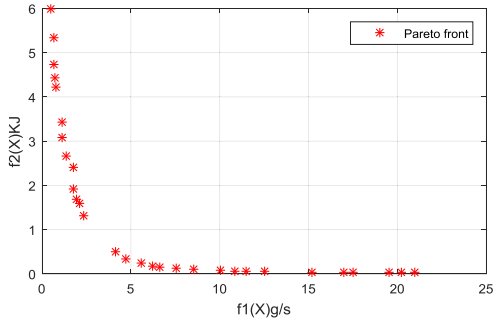

FIGURE 12. The Pareto optimal solutions during the switch process from FWS to RWS.

TABLE 3. The selected optimization results from the Pareto optimal solutions.

Optimization variable X			$f_1(X)(m/s^3)$	$f_2(X)(KJ)$
$\varphi(rad)$	$r(\deg)$	$\Delta t(s)$		
0.20	1.01	0.61	4.15	0.50
1.07	0.45	1.23	1.36	2.66
1.35	0.57	1.34	1.14	3.09
1.05	0.37	1.04	1.77	1.91
0.57	0.93	1.42	1.10	3.44
0.22	1.11	0.87	2.35	1.31
1.05	0.34	0.98	1.95	1.68

B. SWITCH FROM FWS TO RWS

In the switch from FWS to RWS simulation, the longitudinal speed of the vehicle is set as 10 m/s and the road friction coefficient is set as 0.85. The optimal switch trajectory is obtained through the Pareto optimal solutions according to the MOGA based on NGSA-II, and the Pareto optimal solutions are shown in Figure 12.

Some optimization results from the Pareto optimal solutions are selected, which are listed in Table 3.

$X = (1.07, 0.45, 1.23)$ is selected to calculate the control points of the B-spline curve, and then a wheel trajectory of the driving wheel based on the B-spline curve is created, which is shown in Figure 13. Based on the angle relationship

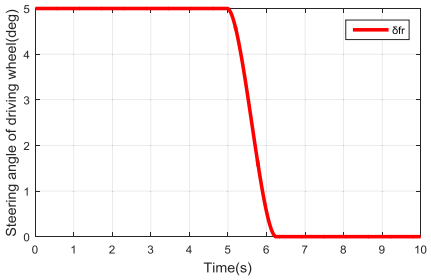

FIGURE 13. The steering angle of the driving wheel under the switch from FWS to RWS.

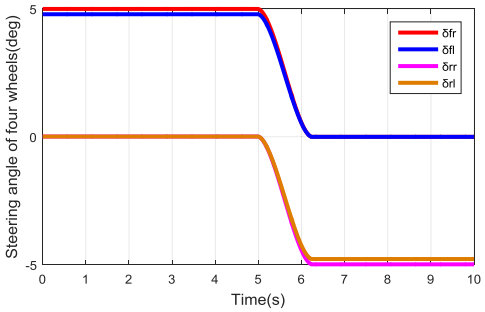

FIGURE 14. The steering angle of four wheels under the switch from FWS to RWS.

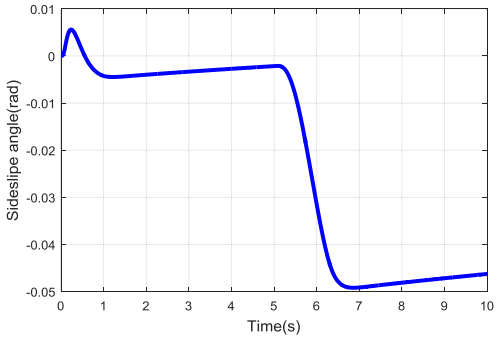

FIGURE 15. The sideslip angle response of the vehicle under the switch from FWS to RWS.

between the driving wheel and the driven wheels, the switch trajectories of four wheels are generated and shown in Figure 14. It can be seen from Figure 14 that the vehicle runs in FWS mode in 0-5s period, and the vehicle is in the switch process in 5-6.23s period, and the vehicle steers in RWS mode in 6.23-10s period. During the switch process of steering mode, the calculated turning radius of the 4WIS fire rescue prototype vehicle remains constant at 35.1m, which realizes the switch control target.

Taking the steering angles of four wheels as the input of the steering system, Figures 15-17 show the dynamic parameters of the vehicle.

As can be seen from Figure 15-16, during the switch process from FWS to RWS, the sideslip angle and the yaw rate of the vehicle change slowly, avoiding the parameter mutation caused by the switch. On the other hand, Figure 17 shows that the smooth lateral acceleration guarantees the roll stability of the 4WIS fire rescue vehicle in the switch process. Hence, the proposed dynamic switch from FWS to RWS is helpful.

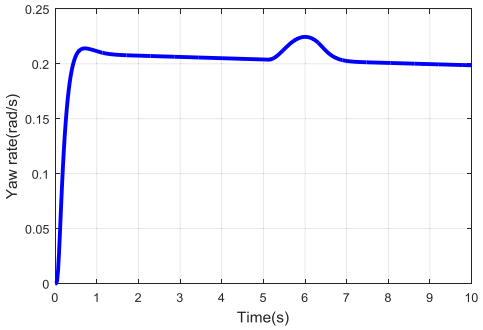

FIGURE 16. The yaw rate response of the vehicle under the switch from FWS to RWS.

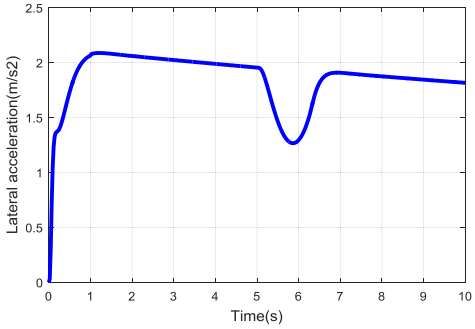

FIGURE 17. The lateral acceleration response of the vehicle under the switch from FWS to RWS.

Based on the simulation results of two typical switches mentioned above, it is concluded that: (1) the MOGA based on NSGA-II can obtain the Pareto optimal solutions and is suitable for optimizing the switch trajectory design based on the B-spline curve; (2) the presented dynamic switch method of steering modes for the 4WIS rescue vehicle in the non-parking state is effective.

V. CONCLUSION AND FURTHER WORK

In order to solve the problem that the 4WIS rescue vehicle must be in the parking state when the steering mode is switched, this paper proposes the dynamic switch method among three steering modes (FWS, RWS and 4WS) for the 4WIS rescue vehicle in the non-stop state. According to the constant turning radius principle, the angle relationships between the three driven wheels and the driving wheel during the switch process are derived, and the target steering angle of the driving wheel is obtained.

Based on the B-spline theory, the wheel trajectories of the steering mode switch for the 4WIS rescue vehicle are constructed. Two optimization objectives including the lateral acceleration's maximum change rate and the tire dissipation energy are built based on the nonlinear 8DOF vehicle model, and a MOGA based on NSGA-II is proposed to obtain the optimal switch trajectories of wheels. The numerical simulations of two typical switches from FWS to 4WS or to RWS are carried out through Matlab/Simulink software. The simulation results show that the MOGA based on NSGA-II can obtain the Pareto optimal solutions and is suitable for optimizing the switch trajectory design based on the B-

spline curve. Furthermore, the proposed switch control strategy of steering modes in the non-stop state is reasonable and effective, which not only avoids the sudden change of the vehicle dynamic parameters, but also ensures the vehicle's roll stability during the switch process.

However, there are still some drawbacks in the proposed switch method which need to be further strengthened.

(1)The steering mode switch experiments will be conducted after completing the design of the fire rescue prototype vehicle.

(2)The optimal B-spline curve based on MOGA is done offline, however, the steering mode needs to be switched real-time. In the next step, the switch trajectory under the different vehicle states needs to be optimized offline, and then these trajectories are fitted and analyzed to obtain the real-time optimal B-spline curve. Finally, the steering mode can be switched real-time.

(3)When the vehicle is in a potentially unstable or dangerous situation before switching to other steering modes, the steering mode cannot be switched, otherwise the hazard of the vehicle will be exacerbated. Therefore, the preconditions for steering mode switch are necessary to be investigated in the future.

ACKNOWLEDGMENT

The authors would like to thank the institute of electrohydraulic control technology for engineering machinery at Jilin University and the Xuzhou Construction Machinery Group Co., Ltd. for supporting this research.

REFERENCES

[1] Y. D. Setiawan, T. H. Nguyen, P. S. Pratama, H. K. Kim, and S. B. Kim, "Path tracking controller design of four wheel independent steering automatic guided vehicle," *Int. J. Control, Autom. Syst.*, vol. 14, no. 6, pp. 1550–1560, Dec. 2016.

[2] P. Hang, X. Chen, S. Fang, and F. Luo, "Robust control for four-wheel-independent-steering electric vehicle with steer-by-wire system," *Int. J. Automot. Technol.*, vol. 18, no. 5, pp. 785–797, Oct. 2017.

[3] Q. Tan, P. Dai, Z. Zhang, and J. Katupitiya, "MPC and PSO based control methodology for path tracking of 4WS4WD vehicles," *Appl. Sci.*, vol. 8, no. 6, p. 1000, Jun. 2018.

[4] X. Y. Tu, "Robust navigation control and headland turning optimization of agricultural vehicles," Ph.D. dissertation, Dept. Agricult. Biosyst. Eng., Iowa State Univ., Ames, IA, USA, 2013.

[5] T. L. Lam, H. Qian, and Y. Xu, "Omnidirectional steering interface and control for a four-wheel independent steering vehicle," *IEEE/ASME Trans. Mechatronics*, vol. 15, no. 3, pp. 329–338, Jun. 2010.

[6] W. D. Esquivel and L. E. Chiang, "Nonholonomic path planning among obstacles subject to curvature restrictions," *Robotica*, vol. 20, no. 1, pp. 49–58, Jan. 2002.

[7] C. Chen, Y. Q. He, and C.-G. Bu, "Feasible trajectory generation for autonomous vehicles based on quartic Bézier curve," *Acta Automatica Sinica*, vol. 41, no. 3, pp. 486–496, 2015.

[8] K. Yang, D. Jung, and S. Sukkarieh, "Continuous curvature path-smoothing algorithm using cubic Bézier spiral curves for non-holonomic robots," *Adv. Robot.*, vol. 27, no. 4, pp. 247–258, Mar. 2013.

[9] C. G. L. Bianco and O. Gerelli, "Generation of paths with minimum curvature derivative with η^3 -splines," *IEEE Trans. Autom. Sci. Eng.*, vol. 7, no. 2, pp. 249–256, Apr. 2010.

[10] T. Berglund, A. Brodnik, H. Jonsson, M. Staffanson, and I. Söderkvist, "Planning smooth and obstacle-avoiding B-spline paths for autonomous mining vehicles," *IEEE Trans. Autom. Sci. Eng.*, vol. 7, no. 1, pp. 167–172, Jan. 2010.

[11] X. Zhang, X. Lu, S. Jia, and X. Li, "A novel phase angle-encoded fruit fly optimization algorithm with mutation adaptation mechanism applied to UAV path planning," *Appl. Soft Comput.*, vol. 70, pp. 371–388, Sep. 2018.

[12] M. Elbanhawi, M. Simic, and R. N. Jazar, "Continuous path smoothing for car-like robots using B-spline curves," *J. Intell. Robotic Syst.*, vol. 80, pp. 23–56, Dec. 2015.

[13] K. Deb, A. Pratap, S. Agarwal, and T. Meyarivan, "A fast and elitist multiobjective genetic algorithm: NSGA-II," *IEEE Trans. Evol. Comput.*, vol. 6, no. 2, pp. 182–197, Apr. 2002.

[14] M. V. O. Camara, G. M. Ribeiro, and M. De C. R. Tosta, "A Pareto optimal study for the multi-objective oil platform location problem with NSGA-II," *J. Petroleum Sci. Eng.*, vol. 169, pp. 258–268, Oct. 2018.

[15] S. Jeyadevi, S. Baskar, C. K. Babulal, and M. W. Iruthayarajan, "Solving multiobjective optimal reactive power dispatch using modified NSGA-II," *Int. J. Elect. Power Energy Syst.*, vol. 33, no. 2, pp. 219–228, 2011.

[16] S. Ramesh, S. Kannan, and S. Baskar, "Application of modified NSGA-II algorithm to multi-objective reactive power planning," *Appl. Soft Comput.*, vol. 12, no. 2, pp. 741–753, Feb. 2012.

[17] S. Bandyopadhyay and R. Bhattacharya, "Solving multi-objective parallel machine scheduling problem by a modified NSGA-II," *Appl. Math. Model.*, vol. 37, nos. 10–11, pp. 6718–6729, Jun. 2013.

[18] H. Asefi, F. Jolai, M. Rabiee, and M. E. T. Araghi, "A hybrid NSGA-II and VNS for solving a bi-objective no-wait flexible flowshop scheduling problem," *Int. J. Adv. Manuf. Technol.*, vol. 75, nos. 5–8, pp. 1017–1033, Nov. 2014.

[19] M. Souier, M. Dahane, and F. Maliki, "An NSGA-II-based multiobjective approach for real-time routing selection in a flexible manufacturing system under uncertainty and reliability constraints," *Int. J. Adv. Manuf. Technol.*, vol. 100, nos. 9–12, pp. 2813–2829, Feb. 2019.

[20] H. Jiang, J. Yi, S. Chen, and X. Zhu, "A multi-objective algorithm for task scheduling and resource allocation in cloud-based disassembly," *J. Manuf. Syst.*, vol. 41, pp. 239–255, Oct. 2016.

[21] A. Ebrahimi and G. B. Loghmani, "Shape modeling based on specifying the initial B-spline curve and scaled BFGS optimization method," *Multimedia Tools Appl.*, vol. 77, no. 23, pp. 30331–30351, Dec. 2018.

[22] C. D. Boor, "On calculating with B-splines," *J. Approximation Theory*, vol. 6, no. 1, pp. 50–62, Jul. 1972.

[23] M. S. Arslan and N. Fukushima, "Energy optimal control design for steer-by-wire systems and hardware-in-the-loop simulation evaluation," *J. Dyn. Syst., Meas., Control*, vol. 137, no. 7, Jul. 2015, Art. no. 071005.

[24] X. Fei-Xiang, L. Xin-Hui, C. Wei, Z. Chen, and C. Bing-Wei, "Improving handling stability performance of four-wheel steering vehicle based on the H2/H∞ robust control," *Appl. Sci.*, vol. 9, no. 5, p. 857, Mar. 2019.

[25] T. Tanaka, C. L. Ayala, Q. Xu, R. Saito, and N. Yoshikawa, "Fabrication of adiabatic quantum-flux-parametron integrated circuits using an automatic placement tool based on genetic algorithms," *IEEE Trans. Appl. Supercond.*, vol. 29, no. 5, Aug. 2019, Art. no. 1301706.

[26] P. E. Mergos and A. G. Sextos, "Selection of earthquake ground motions for multiple objectives using genetic algorithms," *Eng. Struct.*, vol. 187, pp. 414–427, May 2019.

[27] M. Nemati, M. Braun, and S. Tenbohlen, "Optimization of unit commitment and economic dispatch in microgrids based on genetic algorithm and mixed integer linear programming," *Appl. Energy*, vol. 210, pp. 944–963, Jan. 2018.

[28] Y. Censor, "Pareto optimality in multiobjective problems," *Appl. Math. Optim.*, vol. 4, no. 1, pp. 41–59, 1977.

FEIXIANG XU received the M.S. degree from the East China University of Science and Technology, Shanghai, China, in 2017. He is currently pursuing the Ph.D. degree with Jilin University, Changchun, China. His research interests include steer-by-wire systems and four wheel independent steering vehicle.

XINHUI LIU received the Ph.D. degree from Jilin University, Changchun, China, in 1987, where he is currently a Professor. His current research interests include electro-hydraulic proportional control and four wheel independent steering vehicle.

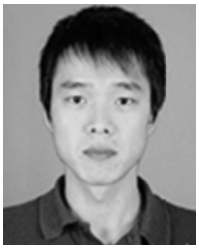

WEI CHEN received the Ph.D. degree from Jilin University, Changchun, China, in 2009, where he is currently an Associate Professor. His current research interests include the development of engineering vehicles and four wheel independent steering vehicle.

CHEN ZHOU is currently pursuing the Ph.D. degree with Jilin University, Changchun, China. Her research interests include steer-by-wire systems and four wheel independent steering vehicle.